FOC *f*/48 Spectrophotometric Calibration

M. Voit, R. Jedrzejewski
June 9, 1997

ABSTRACT

This report describes the effort to calibrate the spectrophotometric efficiency of the f/48 long-slit spectrograph. Our calibration target was the white dwarf star LDS 749B. We stepped the target across the slit at two different positions, three arcseconds apart, in order to characterize the throughput as a function of target location with respect to the slit. The target fell directly into the slit during one exposure at each of the two slit positions, and we used these observations to calibrate the instrument's spectrophotometric efficiency. Vignetting affects the spectrograph's throughput at both of these locations along the slit, and the difference in efficiency between them agrees with the expected vignetting. Measurements of the spectrograph's efficiency when the centroid lies slightly off the slit unexpectedly show greater throughput in the blue.

1. Introduction

The recommissioning of the *f*/48 spectrograph has reintroduced long-slit spectroscopic capability to HST for Cycle 5 GTOs and Cycle 6 GOs. Several previous ISRs have described the geometric correction (FOC-095), wavelength calibration (OSG-FOC-096), and spectrographic rectification (OSG-FOC-097) of this mode. This document discusses the spectrophotometric calibration program. Section 2 introduces the calibration observations (proposal 6198). Section 3 describes the spectral extraction procedure. Section 4 outlines how vignetting corrections are applied. Section 5 calculates the spectrograph efficiency, Section 6 discusses the puzzling behavior of the throughputs when the target's center lies slightly off the slit, and Section 7 presents the third-order efficiency

2. Calibration Observations

The 0.06 arcsecond slit width of the FOC *f*/48 spectrograph, perhaps the smallest ever used for astronomical observations, makes target acquisition an unusual challenge. We must first acquire a target with the *f*/48 camera in imaging mode, then slew the telescope so that the target moves to the fiducial slit position. The precise characterization of the

camera's geometric distortion, described in ISR FOC-095, has made this procedure somewhat more robust, but because the FOC's distortion is time-dependent, acquisition in a single slew is not guaranteed. In order to ensure that we acquired the target optimally for our spectrophotometric calibration, we stepped it across the slit at 0.04 arcsecond intervals at each of the two locations. Table 1 lists the observation set we used for our calibration of the 512 x 1024 format.

Table 1. Spectrophotometric Calibration Observations

Dataset	Target	Exposure Time (sec)	POS TARG (arcsec)	Offset from Slit (arcsec)	Filter
x3l80105t	LDS 749B	357.250	-0.12 , 0.0	-0.04	F305LP
x3l80106t	LDS 749B	357.250	-0.08 , 0.0	0.00	F305LP
x3l80107t	LDS 749B	357.250	-0.04 , 0.0	0.04	F305LP
x3l80109t	INTFLAT	800.000			
x3l8010at	LDS 749B	357.250	0.00 , 0.0	0.08	F305LP
x3l8010bt	LDS 749B	357.250	0.04 , 0.0	0.12	F305LP
x3l8010ct	LDS 749B	357.250	0.08 , 0.0	0.16	F305LP
x3l8010dt	LDS 749B	357.250	0.12 , 0.0	0.20	F305LP
x3l8010ft	INTFLAT	800.000			
x3l8010gt	LDS 749B	497.250	-0.08 , 0.0	0.00	F305LP
x3l8010ht	LDS 749B	697.250	-0.08 , 0.0	0.00	F220W
x3l8010it	LDS 749B	638.250	-0.08 , 0.0	0.00	F150W
x3l8010kt	INTFLAT	800.000			
x3l80205t	LDS 749B	357.250	-0.06 , -3.0	0.00	F305LP
x3l80206t	LDS 749B	357.250	-0.02 , -3.0	0.04	F305LP
x3l80207t	LDS 749B	357.250	0.02 , -3.0	0.08	F305LP
x3l80208t	LDS 749B	357.250	0.06 , -3.0	0.12	F305LP
x3l8020at	INT FLAT	800.000			
x3l8020bt	LDS 749B	497.250	-0.06 , -3.0	0.00	F305LP
x3l8020ct	LDS 749B	697.250	-0.06 , -3.0	0.00	F220W
x3l8020ft	INT FLAT	800.000			

We geometrically corrected, wavelength-calibrated, and rectified these spectrographic images, applying the one-step procedure described in ISR OSG-FOC-097. These corrections and calibrations relied on INT FLATs taken within an orbit of each exposure. Table 2 lists the INT FLATs used to correct these images.

Table 2. INT FLATs used in Correction and Calibration

Exposures	INT FLAT
x3l80105t , x3l80106t , x3l80107t x3l8010at , x3l8010bt	x3l80109t
x3l8010ct , x3l8010dt , x3l8010gt x3l8010ht , x3l8010it	x3l8010ft
x3l80205t , x3l80206t , x3l80207t x3l80208t , x3l8020bt , x3l8020ct	x3l8020at

Simple comparisions of the spectra with each other show straightforwardly that the target was centered in the slit during exposure x3l80106t. This exposure boasts the highest flux levels, and the exposures on either side (x3l80105t and x3l80107t) are virtually identical (see Figure 1). Our conclusion that exposure x3l80205t was centered is more model-dependent. As we will describe in Section 3, this finding rests on the agreement between the throughput difference in exposures x3l80106t and x3l80205t and the vignetting model for the *f*/48 camera.

Figure 1: Raw spectra for spectrophotometric calibration. All have same exposure time (357.25 sec) except for x3l8010gt (457.25 sec); x3l80106t has highest throughoutput.

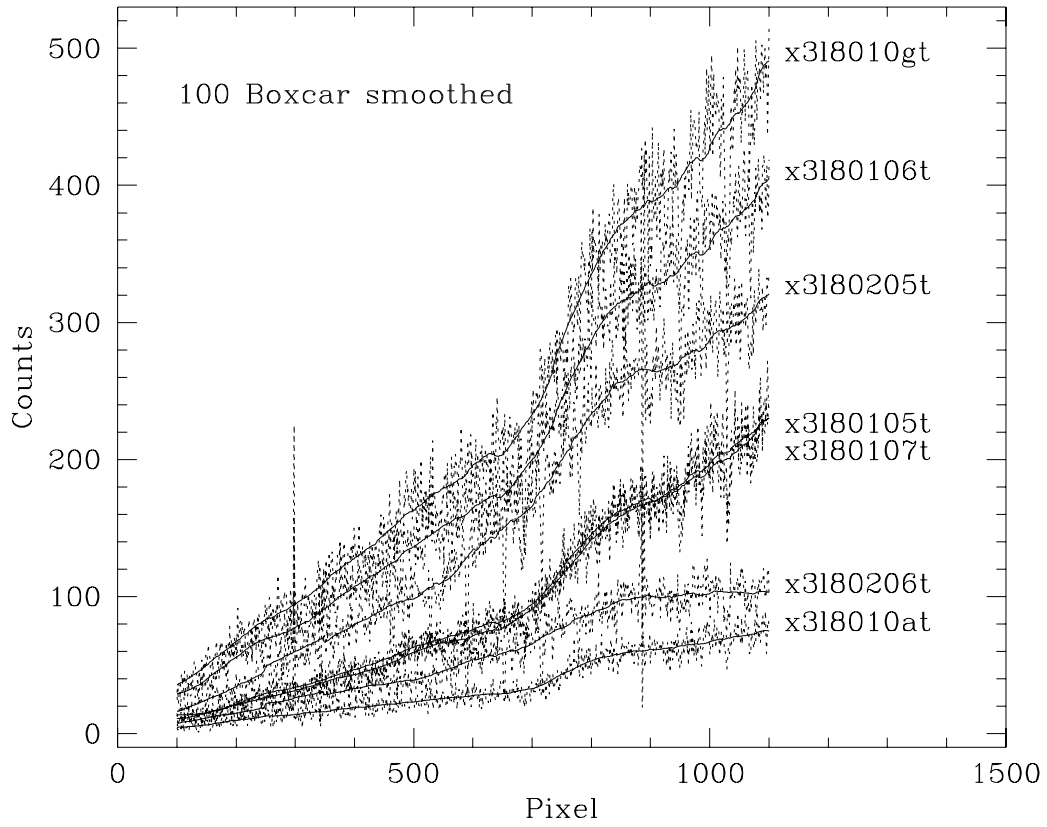

3. Extraction of Spectra

Figure 2 illustrates the 1-D point spread function (PSF) of the spectrograph in the spatial direction. Each line shows the relative counts summed over 200 rows centered on 4000, 4500, and 5000 Å. The full width of the PSF at zero intensity is about 10 pixels, so we chose to extract the spectra within a 10 pixel aperture using the IRAF task `apall`. To remove the background, we subtracted a first-order polynomial fit to the regions between 6 and 10 pixels on either side of the aperture center.

The width of the slit is 0.06 arcseconds, or just slightly larger than 2 pixels. If the PSF in the spectral direction is similar to that in the spatial direction, then the flux through the slit is ~60% of that through a 10 pixel aperture. Thus we estimate that the spectrograph efficiency we will calculate for this point source is only 60% of the value we would calculate for a uniform extended source filling the slit.

Figure 2: One-dimensional point-spread functions in corrected image.

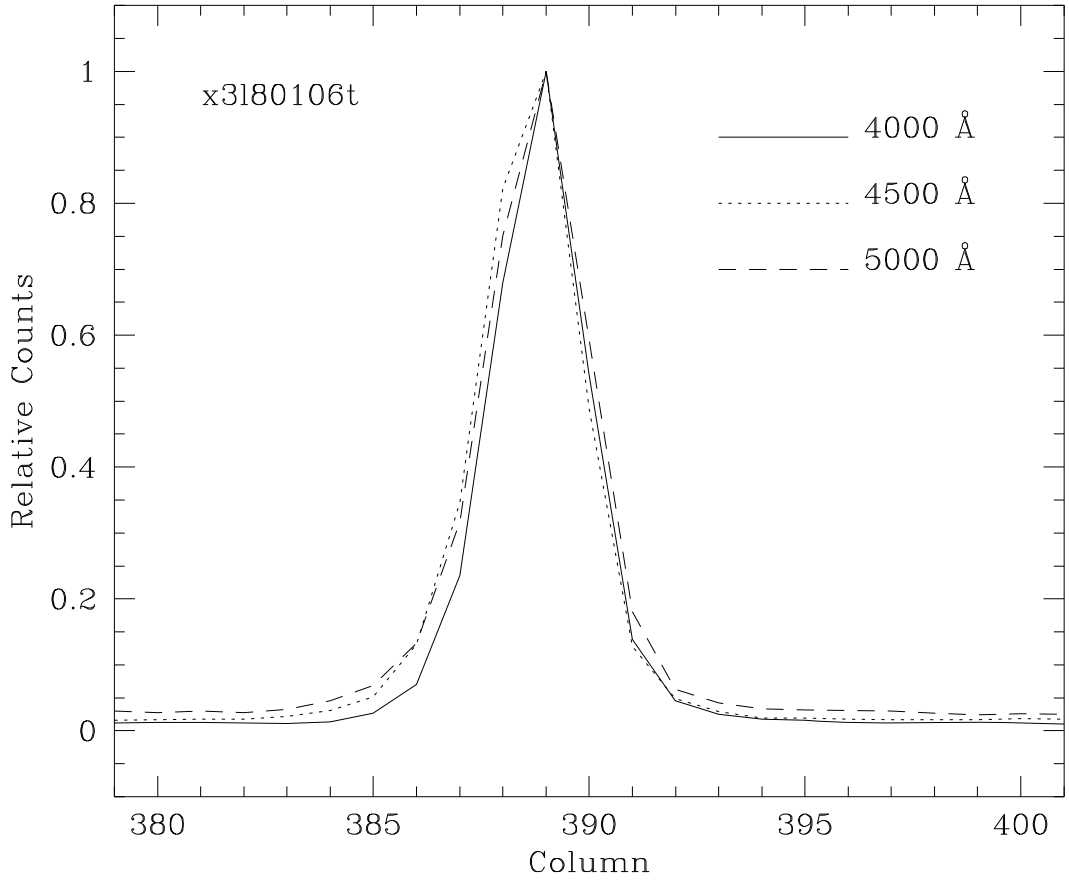

4. Vignetting

One of the few unfortunate side effects of COSTAR has been to introduce vignetting into the FOC *f*/48 camera (see FOC Instrument Handbook for details.) The vignetting increases with increasing *x*-pixel number, beginning 3.5 arcsec from the low-*x* slit end and rising linearly to 50% at the high-*x* slit end. Our spectrum of NGC 6543 in the 512 x 1024 format (see ISR OSG-FOC-096) fills the slit, enabling us to locate the coordinates of the slit ends in a fully corrected image. The slit runs from x = 156 to 575 in this image, so the vignetting model yields following throughput corrections:

$$\begin{aligned} \text{Throughput} &= 1.0 && 156 < x < 278 \\ &= 1.469 - 0.001688x && 278 < x < 575 \end{aligned}$$

According to this model, the sequence of exposures x3l8010*t realizes a throughput of 81.2%, and the sequence x3l8020*t benefits from only 63.5% throughput.

Vignetting accounts quite well for the throughput difference between spectral images x3l80106t and x3l80205t, apparent in Figure 1. Figure 3 shows that the smoothed spectra differ by less than 10% within the calibrated wavelength range (3700-5100 Å). We therefore conclude that image x3l80205t, like x3l80106t, had the target centered in the slit.

Figure 3: Fractional difference between vignetting-corrected spectra x3l80106t and x3l80205t.

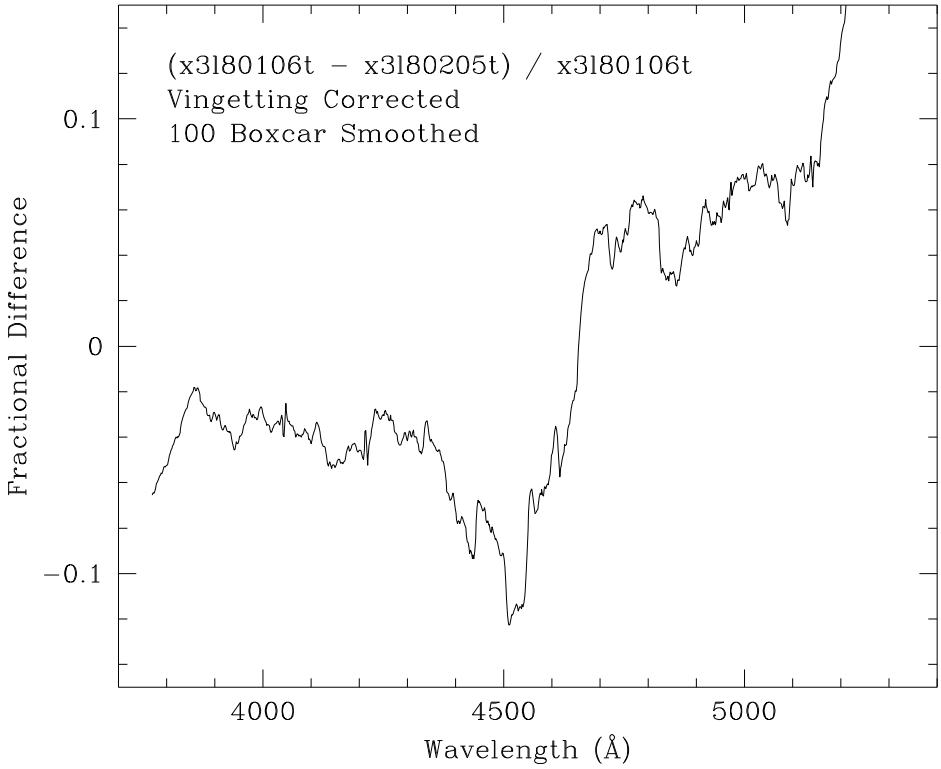

5. Spectrograph Efficiency

To calibrate the *f*/48 spectrograph efficiency, we need to relate the observed spectrum to the tabulated spectrum of the standard star. Figure 4 shows the efficiencies that result when we divide the count spectra by the standard spectrum. We had originally hoped to base this calibration on integration x3l8010gt, which was indended to return the target to its position in x3l80106t. However, the observed efficiency is only 85% of that in the centered image, indicating that the target did not return precisely to slit center. Analysis of the raw images shows that the two spectra are indeed displaced from one another by about 0.5 pixels. We therefore chose to base the calibration on image x3l80106t.

Figure 4: Spectrograph efficiency curves relating counts pixel^{-1} to erg cm^{-2} Å^{-1}..

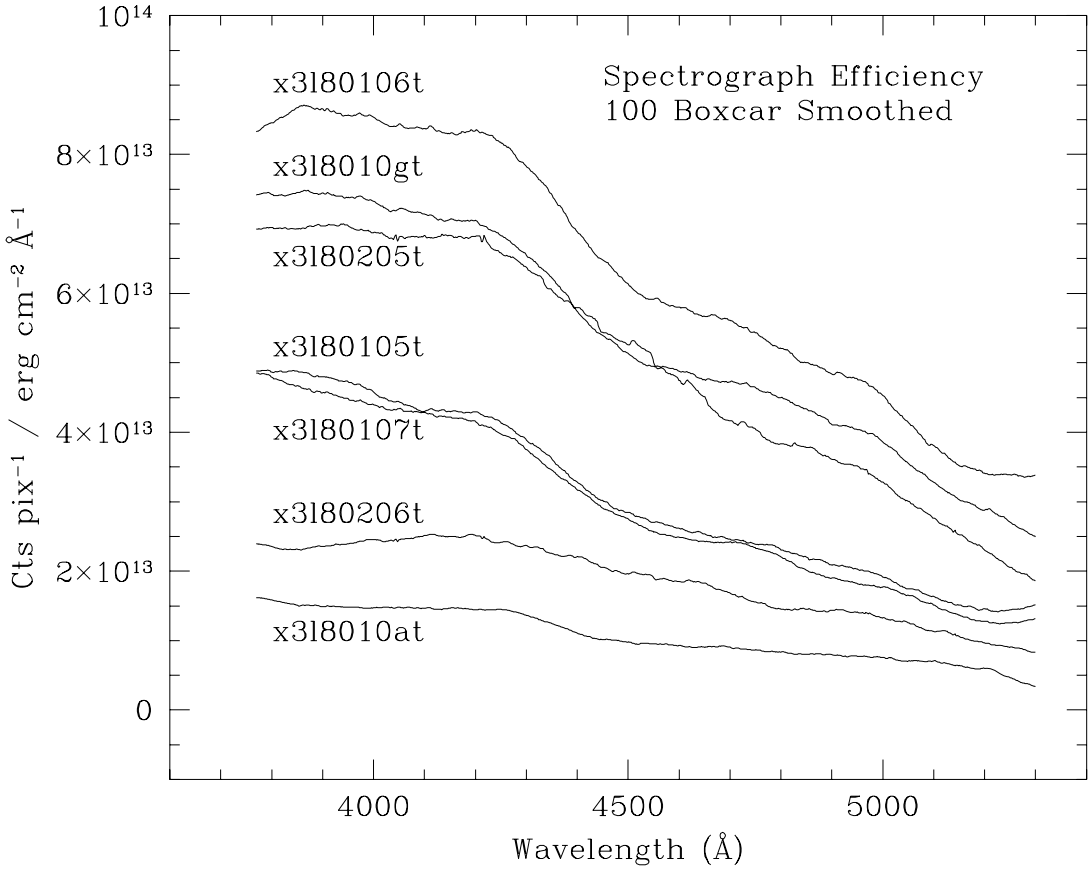

In order to convert the efficiencies in Figure 4 to counts photon^{-1}, we divide by the telescope area, multiply by erg photon^{-1}, divide by the dispersion (1.7 Å pix^{-1}), and correct for vignetting. Taking the additional step of dividing out the point-source throughput of the slit (~60%, see Section 2) yields an estimate of the counts photon^{-1} for extended sources with uniform surface brightness.

Figure 5 compares the efficiencies computed in this way with the predicted efficiency from `synphot`. The dotted line gives the synphot prediction for uniform illumination, and the solid lines show the observed efficiency and the resulting efficiency estimate for uniform illumination. The spectrograph appears to be slightly more efficient than expected in the blue and less so in the red.

Figure 5: Corrected spectrograph efficiency in counts photon^{-1}, based on exposure x3l80106t.

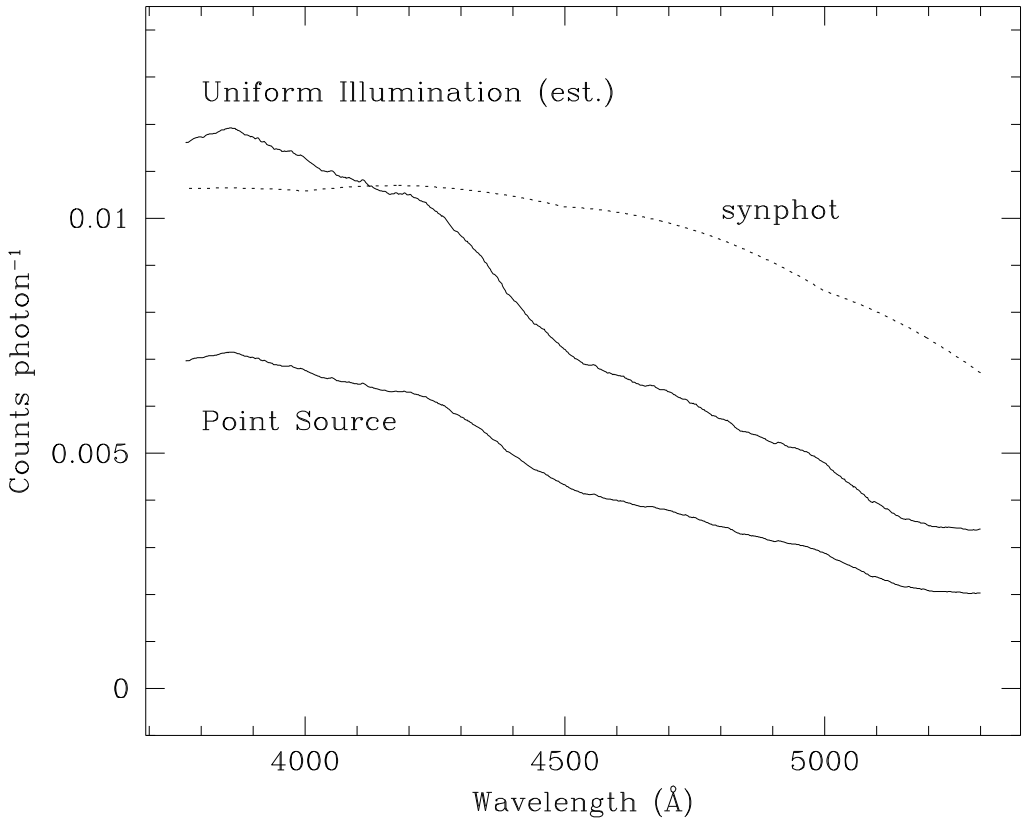

Combining the vignetting-corrected throughput $V(x)$ with the spectral efficiency $E(y)$, in units of (counts pixel^{-1}) / (erg cm^{-2} Å^{-1}), produces a calibration matrix $C(x,y) = [\ V(x) \times E(y)]^{-1}$ valid over an entire FOC image. Multiplying a fully corrected image (corrected as described in ISR OSG-FOC-097) by the matrix $C(x,y)$ yields an image whose pixel values are in units of erg cm^{-2} Å^{-1}. Extracting the spectrum, integrating over the spatial dimension, and dividing by the exposure time gives the spectrum of a point source in erg cm^{-2} s^{-1} Å^{-1}. The pipeline spectrophotometric calibration files for all formats are matrices of the type $C(x,y)$, derived from exposure x3l80106t. In order to suppress the extraneous portions of the image, we set $C(x,y)$ to zero beyond the slit edges and outside of the 3670-5500 Å wavelength range. When working with spectra of extended sources, one must multiply a calibrated file by 0.6 to account for the extra throughput. Figure 6 graphically depicts the matrix $C(x,y)$ for the 512 x 1024 format.

Figure 6: Calibration matrix *C*(*x*,*y*) for the 512 x 1024 format, based on exposure x3l80106t and vignetting model.

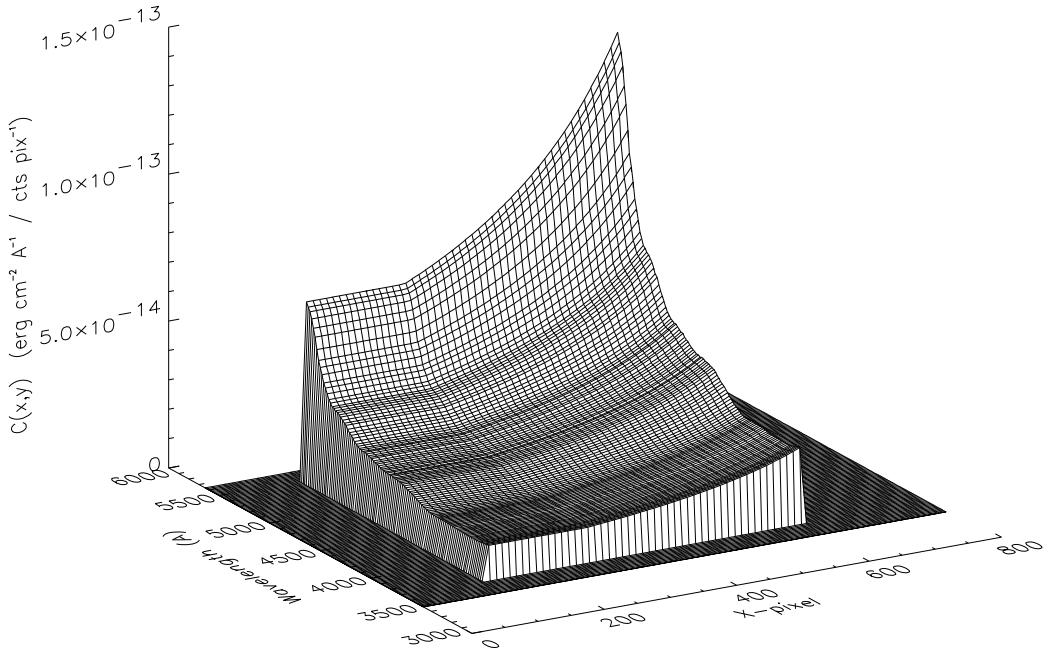

6. Position-Dependent Throughput

The efficiency of the f/48 spectrograph declines as the target moves away from the center of the slit, but this throughput declines in a way that is difficult to understand and to model. Figure 7 shows the efficiency ratios between centered exposures and off-center exposures. The ratios of exposures x3l8010at (0.08 arcsec offset) and x3l8010gt (~ 0.01-0.02 arcsec offset) to x3l80106t are essentially flat, indicating no wavelength-dependence in the throughput. However, similar ratios corresponding to exposures x3l80105t and x3l80107t (0.04 arcsec off center in opposite directions) show that these spectra both increase identically toward the blue relative to x3l80106t. In addition, the ratio of x3l80206t (also 0.04 arcsec offset) to x3l80205t increases slightly toward the red.

An off-center throughput increase toward the red is much easier to understand than an increase towards the blue. We expect the point-spread function of the source to be slightly wider at longer wavelength, so a larger proportion of the flux would fall into an off-center slit. Figure 2 shows that these differences are actually rather subtle; the PSF is probably dominated by imperfect focus rather than diffraction.

Figure 7: Throughput ratios for off-center spectra

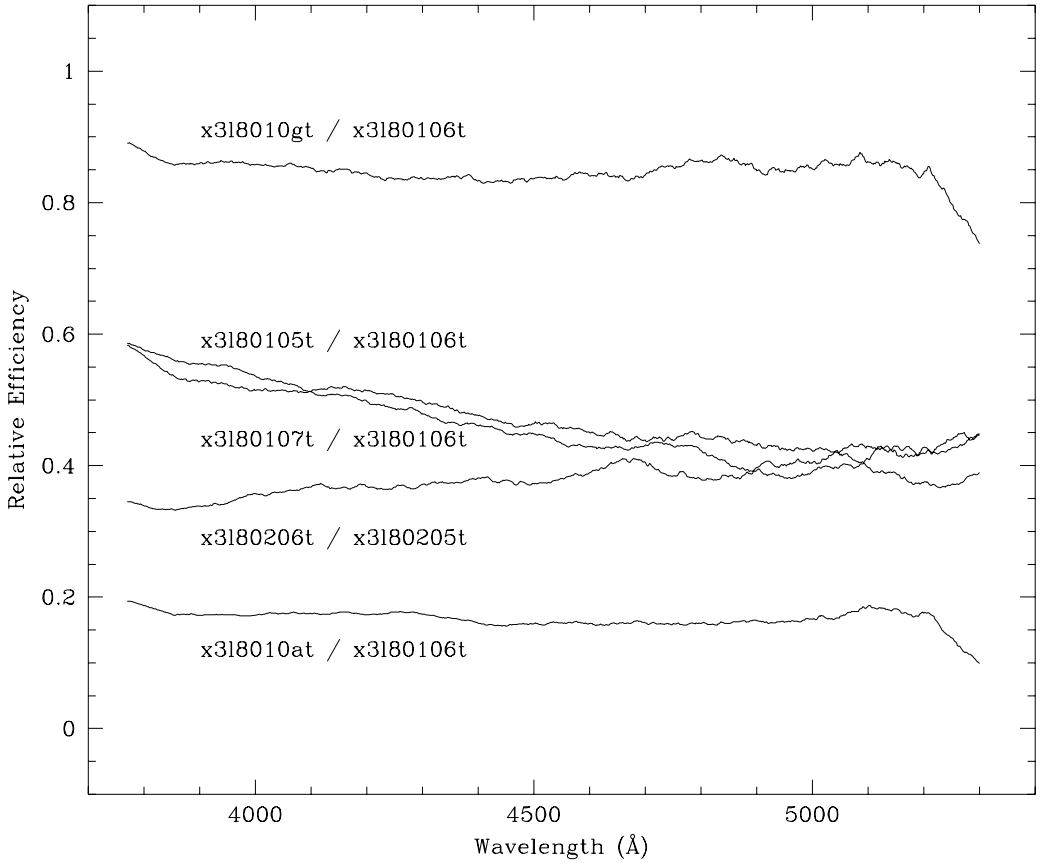

Taking the PSFs in Figure 2 at face value, we can estimate the percentage of flux that would pass through an offset slit 0.06 arcsec wide. At an offset of 0.04 arcsec, the throughput should be ~60% of the centered value, and at 0.08 arcsec the through put should be ~20% of the centered value. Exposure x3l8010at, at an offset of 0.08 arsec, appears to agree with these estimates, but the exposures with 0.04 arsec offsets generally do not, except perhaps at the blue ends of x3l80105t and x3l80107t. The physical reasons for these disagreements between reality and expectations remain murky.

7. Efficiency in Third Order

Spectrographic exposure x3l8010it, taken through the F150W filter, allows us to evaluate the efficiency of the *f*/48 spectrograph in third order, given certain assumptions. First we assume that the throughput in this observation is only 85% of maximum, because it shares the same pointing as exposure x3l8010gt. We also assume that the UV PSF, is identical to the optical PSF, directing 60% of the total flux through the slit. The UV PSF is too noisy to characterize accurately, but it appears to have a similar FWHM. Figure 8 compares the spectrograph efficiencies computed under these assumptions with the predicted

efficiency from `synphot`. They agree to within a factor of 2 over most of the relevant wavelength range.

Figure 8: Corrected spectrograph efficiency in third order, based on exposure x3l8010it